Global Change Biology

Global Change Biology (2013), doi: 10.1111/gcb.12388

Post-clearcut dynamics of carbon, water and energy exchanges in a midlatitude temperate, deciduous broadleaf forest environment

CHRISTOPHER A. WILLIAMS, MELANIE K. VANDERHOOF, MYROSLAVA KHOMIK and BARDAN GHIMIRE

Geography Department, Graduate School of Geography, Clark University, 950 Main Street, Worcester, MA 01610, USA

Abstract

Clearcutting and other forest disturbances perturb carbon, water, and energy balances in significant ways, with corresponding influences on Earth's climate system through biogeochemical and biogeophysical effects. Observations are needed to quantify the precise changes in these balances as they vary across diverse disturbances of different types, severities, and in various climate and ecosystem type settings. This study combines eddy covariance and micrometeorological measurements of surface-atmosphere exchanges with vegetation inventories and chamber-based estimates of soil respiration to quantify how carbon, water, and energy fluxes changed during the first 3 years following forest clearing in a temperate forest environment of the northeastern US. We observed rapid recovery with sustained increases in gross ecosystem productivity (GEP) over the first three growing seasons post-clearing, coincident with large and relatively stable net emission of CO_2 because of overwhelmingly large ecosystem respiration. The rise in GEP was attributed to vegetation changes not environmental conditions (e.g., weather), but attribution to the expansion of leaf area vs. changes in vegetation composition remains unclear. Soil respiration was estimated to contribute 44% of total ecosystem respiration during summer months and coarse woody debris accounted for another 18%. Evapotranspiration also recovered rapidly and continued to rise across years with a corresponding decrease in sensible heat flux. Gross short-wave and long-wave radiative fluxes were stable across years except for strong wintertime dependence on snow covered conditions and corresponding variation in albedo. Overall, these findings underscore the highly dynamic nature of carbon and water exchanges and vegetation composition during the regrowth following a severe forest disturbance, and sheds light on both the magnitude of such changes and the underlying mechanisms with a unique example from a temperate, deciduous broadleaf forest.

Keywords: carbon balance, evapotranspiration, forest disturbance and regrowth, forest management, net ecosystem productivity

Received 16 October 2012 and accepted 5 September 2013

Introduction

Stand-replacing disturbances such as severe fires, severe insect outbreaks, and clearcut's are common agents of change perpetually altering forest resources (e.g., Kurz & Apps, 1999) and contributing an important source of variability at the landscape scale (Cohen *et al*., 1996; Law *et al*., 2004; Turner *et al*., 2007). Severe disturbances perturb a wide range of ecosystem traits such as stand structure, leaf area, species composition, canopy ecophysiology, rates of decomposition and microclimate, with potentially large and long-lasting effects on carbon, water, and energy fluxes (Chen *et al*., 1996, 1999, 2004; Liu *et al*., 2005; Kashian *et al*., 2006; Randerson *et al*., 2006; Amiro *et al*., 2011; Coursolle *et al*., 2012; Ghimire *et al*., 2012; Williams *et al*., 2012). Such disturbance processes typically involve within-class land conversion, that is, 'forest land remaining forest land', and have yet to be incorporated in most earth system models partly because of complexity arising from large site-to-site variability in post-disturbance dynamics (e.g., Turner *et al*., 1999; Kowalski *et al*., 2004; Amiro *et al*., 2011). Quantitative descriptions to date, reviewed below, have tended to focus on temperate and boreal coniferous forests, under representing some important forest types such as broadleaved deciduous forests. Past work has also focused on carbon balance dynamics, thus providing only a partial characterization of the full net radiative effects on the climate system (e.g., Jackson *et al*., 2008). This study quantifies carbon, water, and energy flux dynamics with detailed observations from an intensely instrumented site in a highly dynamic post-clearcut environment undergoing rapid vegetative regrowth typical of a broadleaf deciduous forest in the northeastern USA. The research was conducted within the Harvard Forest Long-Term Ecological Research site (HF LTER).

Correspondence: Christopher A. Williams, tel. + 508 793 7323, fax + 508 793 8881, e-mail: cwilliams@clarku.edu

Forest clearing and natural regeneration are widespread in today's temperate forests of the northeastern USA. Clearcut logging is one of the major causes of stand-replacing disturbances both globally and across much of the United States (Jones *et al.*, 2003; Smith *et al.*, 2009; Miner, 2010). In the northeastern USA, about half of all timberland that experienced cutting from 2001 to 2005 (4884 km^2 yr^{-1}) involved clearcut methods (2394 km^2 yr^{-1}) (Smith *et al.*, 2009; table 43). In central and western Massachusetts, estimates of harvest rates range from 1.4% per year (Kittredge *et al.*, 2003; McDonald *et al.*, 2006) to 2.3% per year (Smith *et al.*, 2009), and are similar to that for heavily managed forests of the southeast and south central regions of the country. Forests naturally recover in many of these clearings, with less than 20% of all harvesting involving conversion (McDonald *et al.*, 2006). Though the average harvesting intensity can be modest in central Massachusetts, with much of the harvesting taking place as selective logging, about one-fifth involves clearcut practices (Kittredge *et al.*, 2003). Furthermore, clearcuts are likely to become more frequent in the future due to growing pressures for biomass energy (Becker *et al.*, 2009). Combined with the expansion of invasive insects such as the hemlock woolly adelgid (Orwig *et al.*, 2008; Nuckolls *et al.*, 2009), Asian longhorned beetle (Haack *et al.*, 2010), and emerald ash borer (Cappaert *et al.*, 2005; Poland & McCullough, 2006) that are resulting in salvage and pre-emptive logging, overall harvesting pressures have grown in recent years.

Flux tower contrasts and age-sequences offer a valuable approach to documenting how carbon, water, and energy balances change with disturbance and recovery processes, though such a sequence has thus far been lacking in a temperate broadleaf deciduous forest environment (Amiro *et al.*, 2000, 2006; Law *et al.*, 2001, 2003; Litvak *et al.*, 2003; Chen *et al.*, 2004; Clark *et al.*, 2004; Binford *et al.*, 2006; Goulden *et al.*, 2006, 2011; Schwalm *et al.*, 2007; McMillan & Goulden, 2008; Zha *et al.*, 2009). A recent paper by Amiro *et al.* (2011) offered an insightful carbon flux synthesis across these sites. They report a general post-harvest net ecosystem productivity (NEP) pattern indicating transition from carbon source to carbon sink over the first decades following stand replacement, often involving relatively constant annual ecosystem respiration (R_{eco}) but a gradual increase in gross ecosystem productivity (GEP). However, between site variability in timing is large, and the early transition from source to sink can be dominated either by a strong decline in GEP that then recovers, or a large increase in R_{eco} that then declines. For example, Florida slash pine and Oregon ponderosa pine chronosequences (clearcut and fire, respectively) showed GEP being relatively constant from 3 to 20 years post-disturbance but R_{eco} generally declining from an early and abrupt post-disturbance increase (Law *et al.*, 2001; Clark *et al.*, 2004). At these sites, roots and coarse woody debris (CWD) may be decomposing more rapidly, or left in larger volume, than at the higher latitude, colder, boreal sites that make up most of the other harvest chronosequences. In another interesting departure from the general pattern, Humphreys *et al.* (2005) found a large rise in GEP in the first 3 years post-clearing that was matched by a corresponding rise in R_{eco} for a Douglas-fir planting on Vancouver Island. Both patterns were attributed mainly to a rapid and sustained expansion of understory growth rather than growth of woody species. Sizable understory regeneration of bamboo played a similarly important role in the rapid rise of GEP following clear-cutting of a cool-temperate, coniferous-broadleaf mixed forest that was replaced with a larch plantation in Japan (Takagi *et al.*, 2009). Studies also report wide variation in the heterotrophic vs. autotrophic contributions to total soil and total ecosystem respiration among post-harvest sites, depending on a combination of factors such as post-cutting management of harvest removals and debris, litter and slash quality, as well as climate. Thus, the precise patterns of GEP and R_{eco} following stand replacement cannot be easily generalized.

Forest disturbances also influence water fluxes, typically decreasing evapotranspiration and increasing runoff (Bosch & Hewlett, 1982). This was clearly demonstrated from deforestation plus herbicide treatments at the Hubbard Brook Experimental Forest in New Hampshire (Likens *et al.*, 1970, 1994). Decades of additional research at the catchment-scale show convincing evidence of reduced runoff from forested catchments compared to adjacent non-forested counterparts (Zhang *et al.*, 2001; Brown *et al.*, 2005; Marc & Robinson, 2007), though the difference declines as forests age (Marc & Robinson, 2007). Similarly, in a global synthesis of afforested sites, Farley *et al.* (2005) reported large average reductions in annual runoff with grassland or shrubland conversion to forests (44% and 31%, respectively). With eddy covariance data from a post-fire chronosequence of boreal Alaska, Liu *et al.* (2005) documented a similar initial decline of evapotranspiration in younger sites and gradual recovery with forest age. Importantly though, such findings are not universal. For example, a review article by Stednick (1996) analyzed changes in annual water yield across paired forested and deforested catchments. The study indicated no detectable change in water yield when less than 20% of a catchment's area was harvested, and some catchments that were completely deforested showed no detectable change in water yield. With the eddy covariance technique, Gholz & Clark (2002) reported equal, if not higher, evapotranspiration post-clearcut compared to neighboring midrotation and rotation-aged slash pine

forests of Florida. These contrasting findings motivate additional study of how evapotranspiration changes following forest disturbances. Evapotranspiration can also provide useful insights into the mechanisms that may be responsible for variation in GEP during the early years following clearing, helping to separate effects of expanded leaf area and canopy conductance from possible effects of a changing microclimate.

Radiation fluxes and energy balance can also be significantly altered by stand-replacing disturbances. For example, Liu *et al.* (2005) documented how the surface energy budget is altered by the legacy of fire with a chronosequence of sites in the interior of Alaska. They reported lower net radiation and lower sensible heat flux, particularly in spring when snow cover and surface albedo varied the most across sites of different ages. Such changes in surface energy fluxes can contribute substantially to the total radiative forcing effects of disturbances, often offsetting the warming effects of CO_2 emissions by increasing surface albedo, especially when disturbances reduce shading of a snow covered surface (Randerson *et al*., 2006). Corresponding analysis has not been performed for clearcut disturbances.

Nearly all prior work examining ecosystem- atmosphere fluxes after forest clearing has been performed in coniferous forests (pine, spruce, or fir), often with plantation treatments rather than natural regeneration (Gholz & Clark, 2002; Kowalski *et al*., 2004; Humphreys *et al*., 2005; Ball *et al*., 2007; Grant 2007; Takagi *et al*., 2009; Zha *et al*., 2009; Coursolle *et al*., 2012). Almost all have emphasized carbon balance dynamics, omitting potentially important variations in water and energy fluxes with post-disturbance recovery. The large and lasting albedo and evapotranspiration legacies reported for post-fire boreal and tundra sites (Liu *et al*., 2005; Randerson *et al*., 2006; Liu & Randerson, 2008; Rocha & Shaver, 2011) have not been examined for post-harvest sites. Quantifying the full dynamics of the coupled cycling of carbon, water, and energy fluxes following clearing will more comprehensively characterize impacts of harvesting and deepen understanding of the drivers of ecosystem physiological changes in the highly dynamic post-clearing environment.

This study's main objective was to quantify the temporal dynamics of water, energy, and carbon dioxide exchanges with the atmosphere in a rapidly and naturally regenerating broadleaf deciduous forest following a clearcut disturbance. We use the first 3 years of data from a flux tower deployed in the Harvard Forest Long-Term Ecological Research (LTER) site to begin addressing the following broad questions:

- How do GEP, R_{eco}, and NEP vary with vegetation recovery in a post-clearcut, deciduous forest environment of the northeastern USA?
- Is there a sustained decrease in evapotranspiration following clearing and how rapidly does evapotranspiration recover with vegetation regrowth?
- How do gross and net radiative fluxes vary seasonally and annually in the early years following forest clearing?

Materials and methods

Site description

The clearcut site is located near the top of Prospect Hill (42.546°N, 72.174°W, elevation 403 m.a.s.l.) within the Harvard Forest LTER site, clearly visible in a color orthophoto of the site from the spring of 2009 (Fig. 1) (USGS Color Ortho Imagery made available from MassGIS (http://www.mass.gov/mgis/colororthos2008.htm). The clearcut site (Fig. 1) was formerly a white and Norway spruce (*Picea glauca* and *abies*, respectively) plantation established between 1916 and 1937, but numerous hardwood deciduous trees and understory herbaceous plants had grown into gaps created by fallen spruce trees. The site was commercially harvested in the fall of 2008 as a clearcut with a mechanical harvester that sheared fine branches and tree tops and cut trees to length, clearing all trees within a roughly 200 × 400 m area (8 ha) except for a few remaining seed trees of mature deciduous species. Many logs were rejected because of low economic value, contributing to a large volume of CWD left to decompose on-site after harvesting. CWD density was estimated by measuring the length and end diameters of all CWD pieces located within nine 20 × 20 m plots spread throughout the clearcut, following methods recommended in Harmon & Sexton (1996). CWD volume per unit area was found to increase from 0.001 m^3 m^{-2} pre-clearcut to 0.024 m^3 m^{-2} post-clearcut (Marshall *et al*., 2011). This large volume of CWD is typical of other clearcut environments in the region (Marshall *et al*., 2011). Soil at the clearcut site is a well-drained Typic Haplorthod (coarse-loamy texture, isotic, frigid) (NRCS, 2010). The monthly mean temperature for Harvard Forest (2005–2010) in January was −4.5 °C and in July was 20.6 °C. The mean annual precipitation, for 2005–2009, was 1355 mm and exhibits only weak seasonality ranging from a minimum monthly total averaging 66 mm in January to a maximum monthly total averaging 125 mm in October (Boose, 2001).

Vegetation cover and composition were assessed with the line-intercept method in late-May to early-June and again in mid- to late-July in each of the second, third, and fourth years following clearing. Five, 50 m transects traversing the clearcut were established and resampled each year, documenting the cover intervals of all plants at a species level. In addition, the species type, diameter, height, canopy width, and number of stems was measured for all seedlings and saplings within 24, 5 × 5 m plots, with each plot surveyed in June and half of the plots resurveyed in July of each year (2010, 2011, and 2012). Species-level leaf area index (m^2 plant species per m^2 ground covered by the species) was also estimated in June to July 2010 with destructive sampling of five to ten individuals of repre-

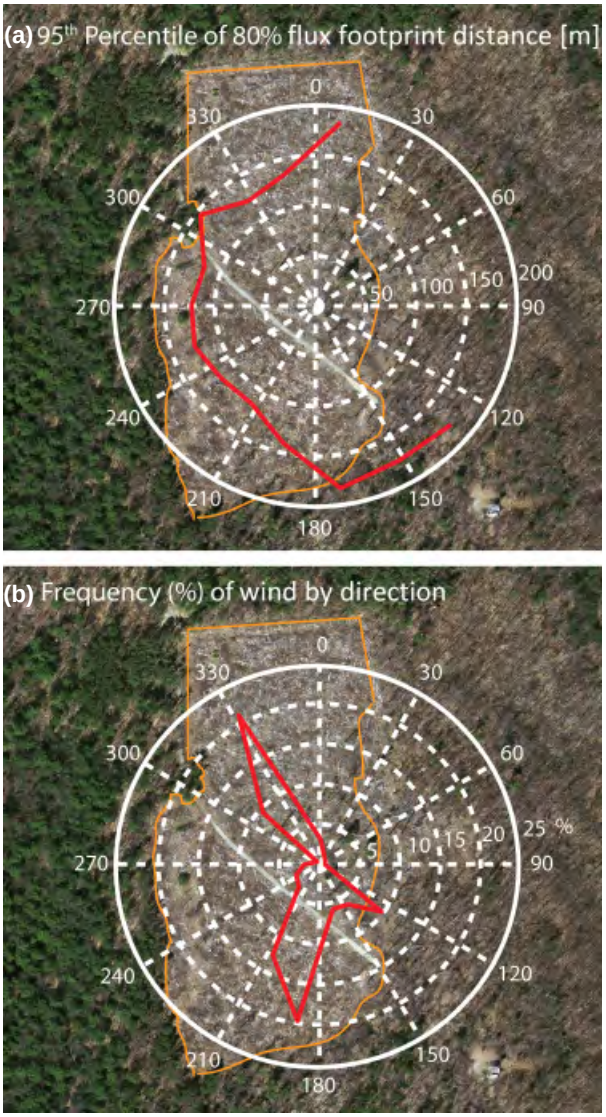

Fig. 1 Flux footprint and wind direction tendencies shown by wind direction and overlaying a color orthophoto of the site in spring 2009 after the clearcut treatment in fall 2008. The irregularly shaped polygon repeated in both panels traces the boundaries of the clearcut. Measurements were conservatively discarded if the mean half-hourly wind direction arrived from 20° to 160°.

sentative stature for each of the major species. The projected area (ground area) occupied by each individual plant was measured, followed by complete removal of its leaves that were then packed tightly but non-overlapping into a box that included a graduated grid from which the total area of leaves for the plant was determined. Vegetation, in the first growing season following the clearcut, was dominated by hay-scented fern (*Dennstaedtia punctilobula*), wood fern (*Dryopteris* spp.), sedges (*Carex* spp.), and starflower (*Treintalis borealis*). Allegheny blackberry (*Rubus allegheniensis*) became a dominant species in the second and third growing seasons, while red maple (*Acer rubrum*) and pin cherry (*Prunus pennsylvanica*) showed an increase in dominance throughout the three growing seasons. Additional results regarding vegetation change across years are reported in Tables 1 and 2.

Measurements and data processing

A 5 m tripod was instrumented with eddy covariance instrumentation including a 3D sonic anemometer (CSAT3; Campbell Scientific, Logan, UT, USA) measuring three-dimensional, orthogonal components of velocity (u, v, w, m s^{-1}) as well as the 'sonic' air temperature (T_a, °C), and an open-path infrared gas analyzer (IRGA, LI-COR LI-7500, Lincoln, NE, USA) measuring concentrations of water vapor (q in g H_2O kg^{-1} air), and CO_2 (μmol CO_2 mol^{-1} air). Starting in mid-June 2009, eddy covariance instruments were installed at 3.0–4.5 m and elevated annually during May to June to maintain a measurement height at or above 1.5 times the canopy height. The tower is located at a local high point of a very gradually sloping landscape. Internal chemicals of the IRGA were changed annually in springtime, followed by zero and span calibrations for CO_2 and H_2O. Calibration gases included Grade−5, 99.999% pure nitrogen for the zero of CO_2 and H_2O, and a NIST traceable primary standard (±1% from Airgas, Inc., Fitchburg, MA, USA) for CO_2 that is confirmed with a secondary standard calibration gas (±0.14 ppm) provided by Ameriflux, and a LICOR dew point generator (LI-610) for H_2O. Post-processing of measured fluxes is described further below.

Average half-hourly incoming and outgoing long-wave and short-wave radiation fluxes (R_{lwin}, R_{lwout}, R_{swin}, R_{swout}) were measured with a Kipp and Zonen (Delft, the Netherlands) CNR1 radiometer mounted at 3 m above the ground, the balance of which provides net radiation (R_n, W m^{-2}). The domes were not heated due to insufficient power supply. Average half-hourly photosynthetically active radiation (PAR, μmol m^{-2} s^{-1}) was recorded with a quantum sensor leveled at 2.5 m above the ground (LI-190SB, LICOR, Lincoln, NE, USA). Additional measurement of air temperature and humidity was recorded with a shielded, solid-state sensor at 2.5 m height (Vaisala HMP45C probe, Campbell Scientific). Average half-hourly volumetric soil water content (θ, m^3 H_2O m^{-3} soil) was estimated with 15 cm long Campbell Scientific (Logan, UT, USA) frequency domain reflectometry probes (CS615) installed horizontally in two separate profiles at soil depths (z, cm) of 10, 25, 50, and 94 cm, or 10, 20, 40, and 80 cm. The probes have not been locally calibrated, and while manufacturer notes suggest absolute accuracy to within 2%, estimates of soil water content are approximate with respect to the absolute water content but nonetheless provide a robust measure of the relative moisture dynamics. Half-hourly averaged soil heat flux (G, W m^{-2}) was obtained with 3 self-calibrating soil heat flux plates (HFP01SC, Hukseflux Thermal Sensors, Delft, the Netherlands) installed 5 cm below the ground surface in representative settings (plant, litter, and coarse woody debris environments). Spatially averaging soil thermocouple probes (TCAV; Campbell Scientific) were installed adjacent to heat flux plates, with probes at 2 and

Table 1 Vegetation characteristics measured in June to July of the first 4 years post-clearcutting (CC). Seedlings refer to woody plants shorter than 1.3 m and with a diameter of 3 cm or less measured 30 cm above the ground, while saplings are taller than 1.5 m

Year	Years post-CC	Vegetation fractional cover May/July	Seedling/sapling stem density (stems m^{-2})*	Mean Tree height/canopy width (cm)	75th percentile/maximum sapling height (cm)	Mean diameter of stems >1 cm (cm)†
2009*	1	0%/40%	0/0	0/0	0/0	
2010	2	66%/70%	4.9/0.1	62/34	165/300	1.3
2011	3	87%/94%	3.3/0.7	89/43	173/285	1.4
2012	4	94%/99%	1.4/1.5	139/62	232/430	1.4

*Numbers for July 2009 are based solely on visual assessment.
†Diameter measured 30 cm above the ground.

Table 2 Species composition ordered by rank abundance (rank of 1 is most abundant) based on areal extent determined with the line-intercept method in July of 2010 and 2011, and associated species-level leaf area index [LAI_{sp}, (m^2 leaf m^{-2} area vegetated by species)] estimated from destructive sampling methods in July 2010

Common name	Scientific name	2009*	2010	2011	Species LAI, 2010 (select)
Knotweed	*Polygonum sp.*	*1*	6	6	2.64 ± 0.86
Hayscented fern	*Dennstaedtia punctilobula*	*2*	13	5	2.27 ± 0.69
Woodfern	*Dryopteris spp.*	*3*	2	7	1.64 ± 0.43
Starflower	*Treintalis borealis*	*4*	11	17	1.23 ± 0.26
Allegheny blackberry	*Rubus allegheniensis*	*5*	1	1	2.25 ± 1.11
Canadian may-lily	*Maianthemum canadense*	*6*	12	16	1
Sweetfern	*Comptonia pergrina*	*7*	27	<30	
Elderberry	*Sambucas pubens*	*8*	10	11	3.28 ± 0.66
Red maple	*Acer rubrum*		3	3	2.81 ± 0.59
Pin cherry	*Prunus pennsylvanica*		4	2	1.47 ± 0.30
Black cherry	*Prunus serotina*		5	9	2.49 ± 0.72
American red raspberry	*Rubus idaeus*		7	4	1.87 ± 1.37
Sedge	*Carex spp.*		8	8	2.68 ± 0.95
Yellow/black birch	*Betula spp.*		9	10	3.32 ± 0.96
White spruce	*Picea glauca*		11	14	2.46 ± 0.53
Striped maple	*Acer pennsylvanicum*		14	19	1.57 ± 0.08
American hornbeam	*Carpinus caroliniana*		16	<30	
Lowbush blueberry	*Vaccinium angustifolium*		17	<30	2.30 ± 0.66
Paper birch	*Betula papyrifera*		18	12	1.40 ± 0.21
Eastern hemlock	*Tsuga canadensis*		19	30	2.43 ± 1.32
White pine	*Pinus strobes*		20	18	3.93 ± 1.20
Red oak	*Quercus rubra*		21	24	1.15 ± 0.20
Wild sarsaparilla	*Aralia nudicaulis*		22	15	1
Serviceberry	*Amelanchier sp.*		23	26	
Dewberry	*Rubus* sp.		24	13	1.55 ± 0.20
Three-leaf goldthread	*Coptis groenlandica*		25	<30	1
Bluebead lily	*Clintonia borealis*		26	21	1

*Presence and approximated rank abundance based solely on visual assessment for 2009.

8 cm below the ground surface. Rainfall per half hour was measured with a tipping bucket precipitation gage (Met One Rain Gage Model 385; Campbell Scientific) located adjacent to the downwind side of the main sensor tripod at 2 m above the ground and in an environment free of elevated obstructions to quantify open field precipitation. However, because the gage was not heated due to insufficient power supply we rely on the Harvard Forest Fisher meteorological station for additional measurements of precipitation (same gage but heated and 1.6 m above the ground in a pasture) recorded as total precipitation delivered over 15 min intervals and available since 2001.

Above-canopy vapor pressure deficit (D_a) was calculated as the difference between the saturation vapor pressure at the air temperature [T_a, (°C)], and the atmospheric water vapor pressure obtained from q and atmospheric pressure [P_a (kPa) recorded by the LI-7500]. Total soil water storage (S, cm) was calculated as the sum of S_i, where

$$S_i = \left\{ \begin{array}{ccc} \theta_1[(z_2 - z_1)/2 + z_1] & for & i = 1 \\ \theta_i(z_{i+1} - z_{i-1})/2 & for & 1 < i < N \\ \theta_N[65 - ((z_N - z_{N-1})/2 + z_{N-1})] & for & i = N \end{array} \right\}, \quad (1)$$

and where N is the number of measurement depths (z). The potential latent energy flux (LE_{pot}, mm d^{-1}) was estimated with the Priestley & Taylor (1972) formulation

$$LE_{pot} = \alpha Q \frac{\Delta}{\Delta + \gamma}, \quad (2)$$

where (α = 1.26) is the Priestley–Taylor coefficient accounting for effects of advection and large-scale entrainment that may elevate potential evapotranspiration above that due to radiation supply, Q is the available energy (W m^{-2} averaged for a half hour period), γ is the psychrometric constant (k Pa K^{-1}), Δ is the slope of the saturation vapor pressure curve evaluated at T_a (k Pa K^{-1}) (Brutsaert, 1982; Campbell & Norman, 1998). Canopy conductance to water vapor (mol H_2O m^{-2} s^{-1}) was calculated with inversion of the Penman–Monteith equation (Monteith, 1965):

$$G_v = \frac{\gamma G_a \Omega}{[\Delta Q + \rho_a C_p D_a G_a]/LE - \Delta - \gamma}, \quad (3)$$

where G_a is the canopy-scale aerodynamic conductance calculated from half-hourly friction velocity [u^*, (m s^{-1})] divided by mean horizontal wind speed (m s^{-1}), ρ_a is the density of air (kg air m^{-3}), M_v is the molecular weight of water (=18.02 g mol^{-1}), C_p is the specific heat capacity of air (J kg^{-1} K^{-1}) (Brutsaert, 1982; Campbell & Norman, 1998), and Ω converts conductance from (m s^{-1}) to (mol m^{-2} s^{-1}) {=44.6*[273/(T_a + 273)]*[P_a/101.3]} (Pearcy *et al.*, 2000). A rectangular hyperbolic light response function was used to parameterize the relationship between GEP and PAR,

$$GEP = \frac{\alpha_p P_\infty \mathrm{PAR}}{\alpha_p \mathrm{PAR} + P_\infty}, \quad (4)$$

where is α_p represents the quantum yield and P_∞ is the asymptotic value of GEP at high light.

Post-processing of the raw high frequency (10 Hz) data for calculation of above-canopy, half-hourly turbulent fluxes of sensible heat (H, W m^{-2}), water vapor (LE, W m^{-2}), and carbon dioxide (F_c, mg CO_2 m^{-2} s^{-1}) was consistent with methods described in Lee *et al.* (2004). It first involved spike filtering based on instrument diagnostics, logical limits, and based on a 4 SD threshold within 3-min data windows. The velocity field was rotated with the planar method of Wilczak *et al.* (2001) applied to monthly data for 30 degree sectors. We corrected sonic temperature to air temperature according to the work of Schotanus *et al.* (1983). LE and F_c were corrected with the Webb–Pearman–Leuning correction (Webb *et al.*, 1980) plus an additional term accounting for surface heating of the instrument (Burba *et al.* 2006). Frequency response correction of some of the energy lost due to instrument separation and gas analyzer response for LE and F_c was performed with empirical cospectral adjustment to match the H cospectrum (Eugster & Senn, 1995; Su *et al.*, 2004). Heat and mass fluxes were calculated with conventional equations (see e.g., Moncrieff *et al.*, 1997; Aubinet *et al.*, 2000). Net fluxes (LE, H, F_c) are reported as positive when from the land to the atmosphere. Lacking measurements of the vertical profile of CO_2 concentration and expecting a modest storage flux given the ecosystem's low stature, we assumed that net ecosystem-atmosphere CO_2 exchange (NEE) equals measured F_c. Lateral and drainage flows of carbon toward groundwater, rivers, and streams can also be important for the net carbon balance of landscapes (Butman & Raymond, 2011; Lauerwald *et al.*, 2012) and may be particularly important following forest disturbance (Schelker *et al.*, 2012). However, such fluxes have not been measured in this work which has a central focus on ecosystem carbon exchange with the atmosphere.

Turbulent flux data were excluded based on instrument diagnostics, data exceeding logical bounds, inappropriate wind direction, low turbulence, and large flux footprint extent. Table 3 summarizes the fraction of data retained after each progressive filter following the approach of Stoy *et al.* (2006). The instrument filter ensures proper sonic anemometer and IRGA function. The logical filter removes unrealistic data points. The wind direction filter removes samples unrepresentative of the clearcut as well as flows that may be adversely influenced by the tower-related hardware itself, conservatively defined as a mean half-hourly wind direction arriving from 20° to 160°. Outside of these sectors fluxes were seen to vary little with wind direction (Fig. S1). The friction velocity filter removes measurements taken when turbulence was not developed well enough to ensure adequate measurement of the surface-atmosphere exchange during the measurement interval. Insufficient turbulence was defined with the method of Papale *et al.* (2006), which identifies the friction velocity above which the measured nighttime CO_2 flux is within 90% of that measured in conditions of even greater turbulence as the median across 6 levels of temperature. The threshold was separately determined for 3 month segments of data identifying a u^* threshold and ranged from 0.12 to 0.18 m s^{-1} (Fig. S2). The extent of the flux footprint was estimated with the analytical flux footprint model of Hsieh *et al.* (2000) and indicates that a source area within 150 m upwind of the tower contributed 80% of the measured flux 95% of the time, well

Table 3 The percentage of turbulent flux data remaining after progressive data filters

	Daytime			Total		
Filter	Fc	LE	H	Fc	LE	H
Instrument	96.3	96.3	96.3	96.2	96.2	96.2
Logical	85.6	88.5	96.3	84.7	87.9	96.2
Wind Direction	81.7	83.6	90.3	79.5	81.8	88.8
Turbulence	68.2	69.3	74.9	56.2	57.3	62.8
Footprint	67.8	68.8	74.3	54.9	55.9	61.5

within the clearcut area (Fig. 1). Measurements were excluded when the 80% flux footprint extended beyond an upwind distance of 200 m and into the land cover types surrounding the clearcut target. Energy balance closure, defined as (H + LE)/(R_n-G), averaged 62% for half-hourly data (intercept of 12.5 W m^{-2}) and 74% for the daily time scale (intercept of 0.85 W m^{-2}). Lack of closure is a well-known chronic issue with the eddy covariance method, but even so this site's closure is lower than the norm. It is not clear to what this can be attributed though the large volume of coarse woody debris may contribute a sizable capacity to store and release energy, a term that is not measured.

Net ecosystem CO_2 exchange (NEE) was separated into ecosystem respiration (R_{eco}) and gross ecosystem productivity (GEP) with the approach of Reichstein *et al.* (2005). Briefly, this approach equates valid nighttime NEE observations with nighttime R_{eco}, derives temporally varying (15-day) empirical coefficients relating R_{eco} to temperature with the Lloyd & Taylor (1994) model, applies the model to estimate a continuous series of R_{eco}, and calculates GEP from R_{eco} − NEE.

Data gaps were filled with the Marginal Distribution Sampling approach of Reichstein *et al.* (2005). This approach replaces missing values with the mean of temporally local, valid flux measurements under analogous environmental conditions (R_{swin}, T_a, D_a). The size of the data window is progressively expanded until filling is successful up to a maximum window size, here up to 2 weeks. Gap-filling, though possible beyond the 2 week window, was deemed to be of low confidence and thus excluded. We only retained values classified as high confidence (class A) by the quality control rating in [Reichstein *et al.* (2005), see appendix A therein].

Carbon dioxide releases were also measured from CWD and soil plots during summer field campaigns using portable, chamber-based instruments (LI-6200, LI-COR, Lincoln Nebraska) (Vanderhoof *et al.*, 2013). The rate of CO_2 release from CWD was measured *in situ* under ambient conditions on sixteen sample logs cut to 50 cm in length with a range of diameters 8–20 cm. Each was placed one at a time inside an air tight plastic chamber with a wire rack at the bottom of the chamber and with an internal fan to provide good air circulation around the log and through the chamber (Liu *et al.*, 2006; Gough *et al.*, 2007). An LI-6200 infrared gas analyzer (IRGA) pumped air through the chamber in a closed loop at a set rate. The CO_2 concentration was recorded every 10 s until a rise of 50 ppm CO_2 was recorded relative to the starting concentration, or until 900 s had passed, whichever was first. To avoid the effects of air disturbance caused by opening the chamber cover, data for the first 45 s after the start of measurements was not used (Jomura *et al.*, 2007). Log-level respiration was calculated as grams of CO_2 emitted per unit of wood surface per unit of time (Hagemann *et al.*, 2010). Soil respiration was also measured in the summers of 2011 and 2012, with the chamber method. Sixteen PVC collars (diameter = 25.4 cm, 20 cm deep) were installed at the site and a LI-6200 IRGA was used to record the rate of soil respiration. In spring 2012, three of the sixteen collars were installed on trenched plots (1 × 1 × 0.3 m deep), where all vegetation was removed. The plots were covered with landscape cloth to prevent herbaceous regrowth. The difference between trenched and untrenched soil respiration rates was used to estimate the autotrophic/heterotrophic partitioning of total soil respiration.

Results

Gross ecosystem productivity (GEP) increased markedly with each year following the clearcut (Fig. 2). During the middle of the growing season typical midday rates equaled 13, 17, and 22 micromoles CO_2 m^{-2} s^{-1} in 2009, 2010, and 2011 (Fig. 2), respectively, indicating a 1.7-fold increase from the first to third year post-clearing. With no appreciable change in short-wave radiation flux or ambient air temperature (Fig. 2), the observed increase in GEP with time since clearing does not appear to be the result of meteorological differences and instead suggests an increase in physiological potential for carbon assimilation. Focusing on the summer season, precipitation and soil moisture were lower in 2010 than the other years (Figs 3 and 4), particularly during the late summer (August, biweeks 16–19), and this was commensurate with elevated vapor pressure deficit (Fig. 2). While it is possible that this contributed to lower August GEP in 2010 compared to 2011, soil moisture and D_a were similar in other months, while GEP was clearly higher in 2011. Also worth noting is a wetter than normal June in 2009 (Fig. 3), which led to sustained high soil moisture during the early summer and lower D_a (Fig. 2), but this did not translate into higher GEP in 2009 (Fig. 2) due to the low leaf area.

The springtime rise in GEP from near zero wintertime values began as early as the 12th week of the year, corresponding to late-March. This was noticeably earlier than in the neighboring mature deciduous broadleaf forests but similar to that for neighboring hemlocks (Wofsy *et al.*, 1993; Goulden *et al.*, 1996; Hadley *et al.*, 2008) and likely due to earlier leaf out of the herbaceous and shrubby functional types in the early successional, post-clearcut environment. Maximal rates of GEP were achieved by around the 24th week of the year, or mid-June and tended to remain fairly stable until mid- to late-August (34th week of the year) when senescence initiated a seasonal decline in GEP. Higher GEP in 2011 compared to 2010 and 2009 persisted from the summer to autumn seasons. Still, by the end of the first growing season post-clearing, GEP was already as high as that in the following year (compare autumn 2009 and 2010 in Fig. 2).

Latent energy flux also increased markedly with time since clearing (Fig. 2). Typical midday water flux rates were 120, 190, 240 W m^{-2} during the midgrowing seasons of 2009, 2010, and 2011, respectively, indicating a doubling from the first to third years after clearing. A

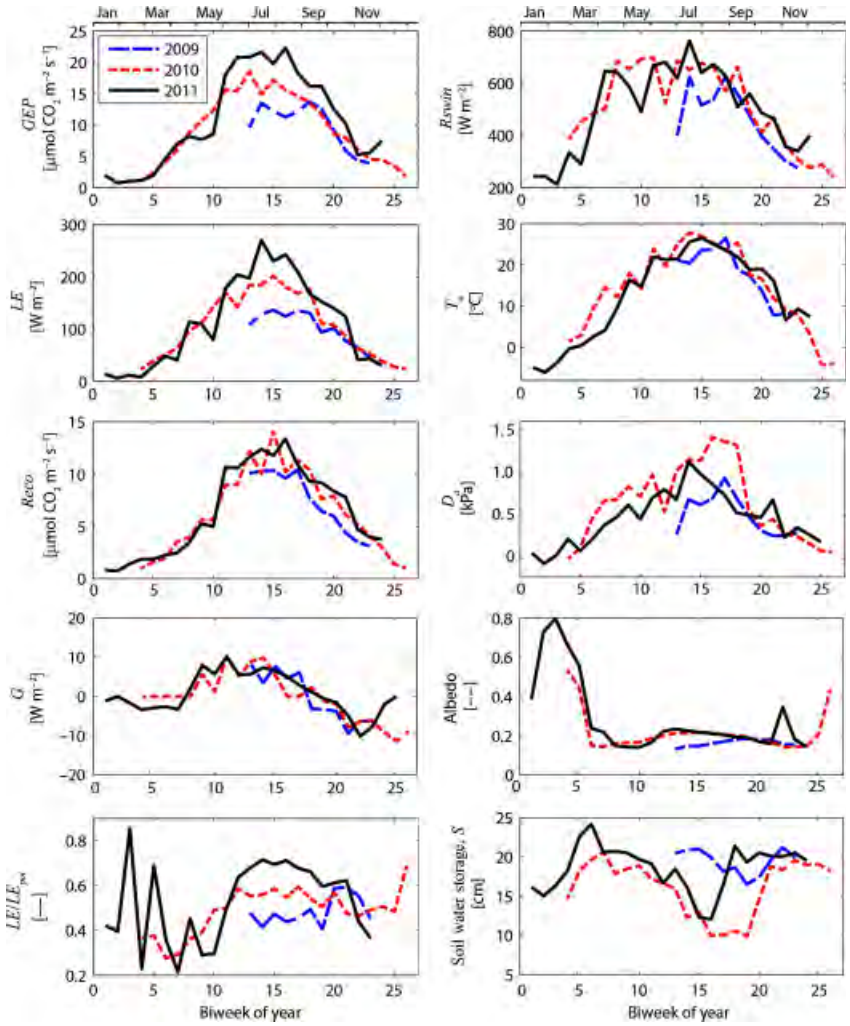

Fig. 2 Mean biweekly fluxes and environmental conditions measured during the daytime hours of 10:00 hours to 13:00 hours for the 3 years following clearcutting.

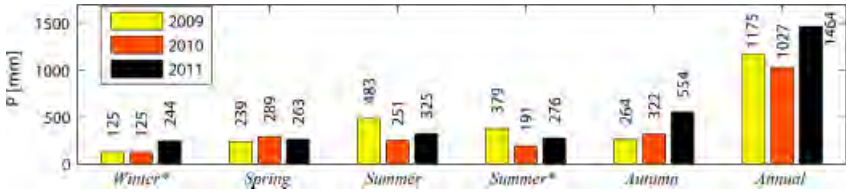

Fig. 3 Cumulative seasonal and annual precipitation for the first 3 years post clearcutting where biweeks included in each season are Winter 1–5 and 24–25, Spring 6–11, Summer 12–17, Summer* 13–17, Autumn 18–23, and Annual 4–25.

similar rate of increase is seen for evaporative fraction (the ratio of actual to potential LE) (Fig. 2), noting that cold season ratios are misleading because of vanishing fluxes. This indicates that the pattern of LE increase over time cannot be attributed to differences in meteorology and instead resulted from increased canopy conductance to water vapor as evidenced further below. The seasonal pattern of LE closely resembled that of GEP.

Ecosystem respiration exhibited relatively subtle variation between years, if any. Mid-growing season R_{eco} was typically 10, 12, and 12 micromoles CO_2 m^{-2} s^{-1} across years at corresponding midday temperatures of 23–26 °C, with a persistent, yet modest elevation of

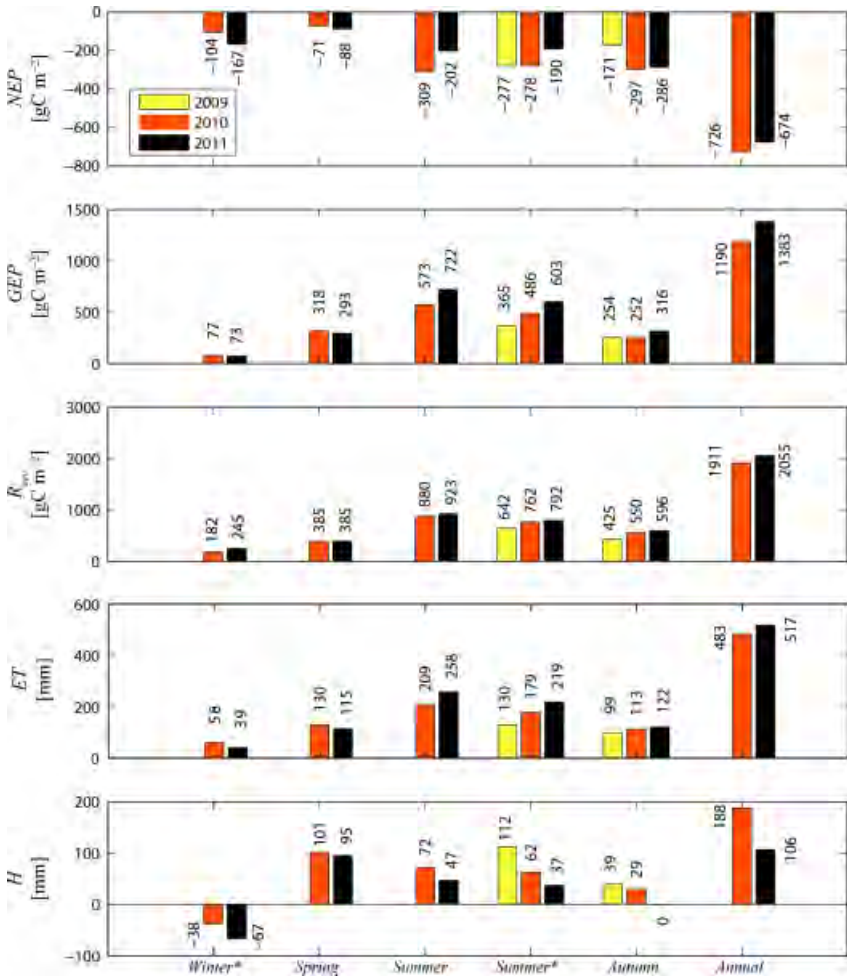

Fig. 4 Cumulative seasonal and annual carbon, water, and energy fluxes for the first 3 years post clearcutting where biweeks included in each season are Winter* 4, 5 and 24, Spring 6–11, Summer 12–17, Summer* 13–17, Autumn 18–23, and Annual 4–25. Winter results are rescaled (x 7/3) to reflect 7 biweeks of results.

2011 rates over those of 2009. Considering that respiration releases continue into nighttime hours, unlike productivity, it is worth noting the sizable ratios of midday R_{eco} to GEP, approximately 0.77, 0.71, and 0.55 for the first 3 years post clearing.

The clearcut site released a large amount of carbon to the atmosphere in each of the years of study (Fig. 4). Net releases tended to be largest in summertime despite sizable GEP. This was true even in 2011, when annual GEP totaled almost 1400 g C m^{-2}, but was overwhelmed by massive R_{eco} exceeding 2000 g C m^{-2} and resulting in a net release of nearly 700 g C m^{-2}. NEP was also strongly negative in the autumn season, because of a larger seasonal decline in GEP compared to that for R_{eco}. Modest respiration releases were seen to continue even into wintertime.

The clearcut site released just less than 500 mm of water to the atmosphere via evapotranspiration (ET) in 2010, and slightly more in 2011 (Fig. 4). Summer season ET accounted for about 40% to 50% of the annual total, while spring and autumn contributions accounted for 20% to 30% each. With annual precipitation of around 1108 mm in 2010 (Fig. 3), this indicates an ecosystem water yield of 625 mm yr^{-1} (1108–483), or a runoff ratio of ca. 0.56 (=625/1108).

Elevation of LE with time since clearing was evident in summer and autumn. This pattern was consistently matched by a corresponding decline in sensible heat flux (H) (Fig. 4). There was a marked reduction in H between years, particularly in the summer season when the Bowen ratio (here H/ET) declined from nearly 1.0 in 2009 to only 0.17 in 2011. Also of note were the negative sensible heat fluxes in the winter season, logically owing to a snow-covered surface cooler than the near surface air such that it is a sink for atmospheric heat.

Radiation fluxes varied little between years (Fig. 5). Season-wide net short-wave radiation flux was stable across years for the summer and autumn seasons, indi-

cating the relatively constant albedo during the first 3 years after clearing (Fig. 2). Net long-wave radiation flux was also largely stable during these seasons. Thus, net radiation varied little between years. During winter, net short-wave radiation flux was much lower (Fig. 5) due to reduced insolation (Fig. 2) as well as higher albedo when snow covered (Fig. 2). Wintertime net long-wave flux was similar to that in other seasons (Fig. 5). However, interpretation of wintertime fluxes should be treated with caution because sensor and power problems during the winter season led to intermittent sampling (see Fig. 2). As with R_n, soil heat flux (G) varied little between years (Fig. 2) though the expected seasonal pattern is evident, with flux into the ground during the warm season and release out of the ground during the cold season.

The strong increase in GEP across years results from an elevated CO_2 fixation rate per unit of incident photosynthetically active radiation (PAR) (Fig. 6). Light response curves indicate a large rise in GEP for a given light-level, with the median rate in 2011 resembling or exceeding the 99th percentile in 2009 and the median rate in 2009 resembling the 1st percentile in 2011. This pattern appears strongly in the multi-year rise in light response parameters, including both quantum yield as well as the asymptotic maximum photosynthetic rate each inferred from fitting a rectangular hyperbolic function (Table 4). It is unclear if this multi-year trend is because a larger fraction of incident PAR is absorbed by an expanding canopy, or if the ecosystem's leaf-level potential to assimilate CO_2 has increased over years. Both would be plausible. Sizable increases in leaf area and vegetation cover are being recorded at the site (Tables 1 and 2). Preliminary analysis of leaf-level gas exchange data indicate large species level differences in

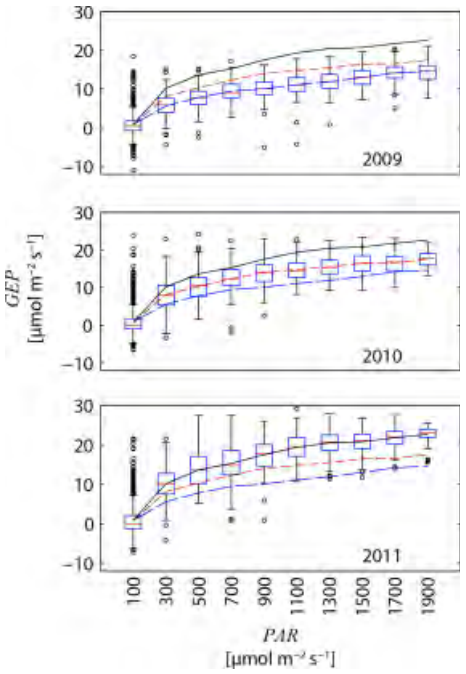

Fig. 6 Midgrowing season light response curves expressed as boxplots. Curves indicate medians for 2009 (blue, long dash), 2010 (red, short dash), and 2011 (black, continuous). Boxes span the 25th to 75th percentiles, while whiskers span ±2.7 times the SD (or roughly the 1st to 99th percentiles). Midgrowing season is defined as the 12th to 17th biweeks of the year, or June to mid-August.

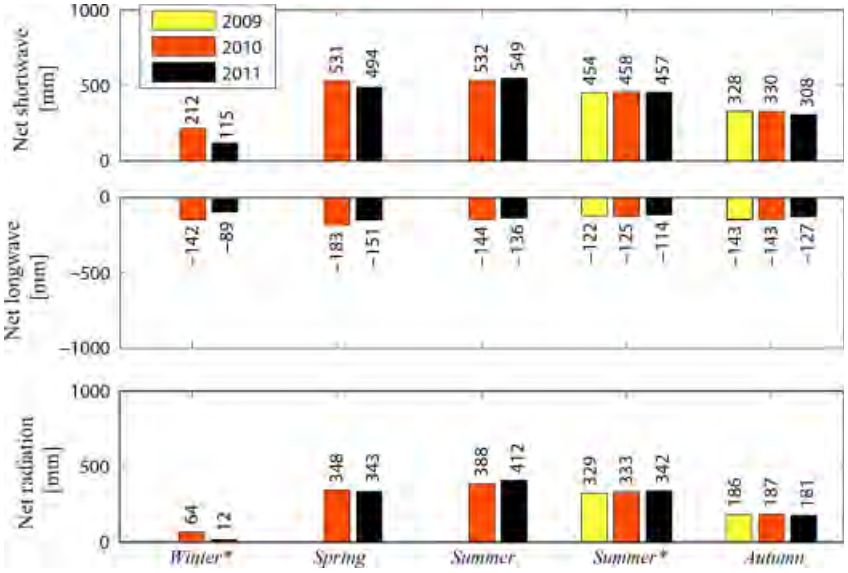

Fig. 5 Cumulative seasonal net radiation fluxes for the first 3 years post clearcutting where biweeks included in each season are Winter* 4, 5, and 24, Spring 6–11, Summer 12–17, Summer* 13–17, Autumn 18 to 23. Winter results are rescaled (x 7/3) to reflect 7 biweeks of results.

Table 4 Light response curve parameters for midgrowing season data in each year obtained in the rectangular-hyperbolic fits of GEP vs. PAR. Standard deviations on the parameters were obtained from 50 bootstrap replicates involving random resampling of 90% of the data with replacement

	2009	2010	2011
α_p	0.0279 ± 0.0004	0.0452 ± 0.0005	0.0529 ± 0.0005
P_∞	18.63 ± 0.15	21.27 ± 0.13	28.57 ± 0.13
R^2	0.88	0.91	0.93

assimilation rate, with vegetation compositional shifts and leaf area trending toward species with greater physiological potential for carbon fixation.

The sizable increase in LE across years is consistent with elevation of the rate of canopy conductance to water vapor (G_v) (Fig. 7). From inverting the Penman–Monteith model of evapotranspiration (Monteith, 1965), we calculated instantaneous rates of water vapor conductance at the canopy scale. Mid-growing season, midday G_v increased each year, with a large increase from 2010 to 2011. The rise in conductance between years is consistent across time of day despite the typical afternoon decline in conductance due to diurnal depletion of plant water stores and elevated vapor pressure deficit in the afternoon. The rise in conductance over years cannot be attributed to a trend in vapor pressure deficit itself between years because there is a clear rise in canopy conductance for a given level of D_a, both in the morning and afternoon (Fig. 8). As with the noted multi-year rise in GEP/PAR, it remains unclear if the trend in conductance results from vegetation structural changes, such as an expanded exchange surface ($LAI_{sp} \times f_{veg}$) and more extensive root systems, or rather a compositional shift in canopy physiology, in this case toward more water-use-intensive species.

The multi-year rise in both GEP and LE are reflected in midgrowing season P_∞ and G_v, respectively. Plotting these parameters vs. f_{veg} and (LAI_{sp} x f_{veg}) reveals nonlinear relationships, with a steeper rise from 2010 to 2011 compared to 2009 to 2010 (Fig. 9). Comparison to values obtained at a nearby mature hardwood forest (Harvard Forest Environmental Monitoring Station less than 1 km away, based on Urbanski *et al.* (2007)) suggests that a further rise in productivity is possible. However, it is notable that after only 3 years following clearcutting the site is already reporting rates of productivity comparable to the low end of the range for the nearby mature forest (75–100 year old) dominated by oak and maple trees. This between-site comparison also suggests that additional layers of leaves with continued post-clearcut regrowth will yield a less than proportional increase in GEP, consistent with self-shading and overall light-limitation.

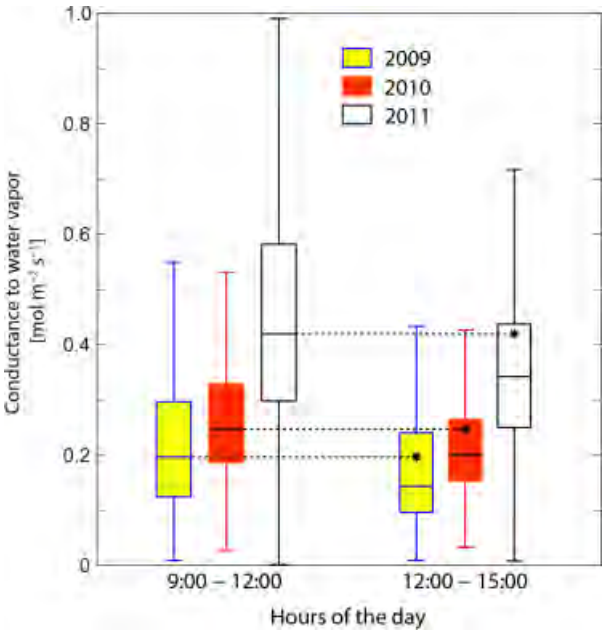

Fig. 7 Midgrowing season conductance to water vapor during morning and early afternoon hours in the 3 years post clearcutting expressed as box plots (as in Fig. 7). Conductance was calculated with inversion of the Penman–Monteith equation. Mid growing season is defined as the 12th to 17th biweeks of the year.

Discussion

Productivity recovered quickly but not enough to offset respiration, which remained large and relatively stable across years. This pattern was consistent with the recent synthesis of flux tower data by Amiro *et al.* (2011), which arrayed data from various forest types by each site's time since disturbance to study the broad temporal trajectory of carbon fluxes following stand-replacing disturbances. They reported a general post-harvest pattern of relatively constant annual ecosystem respiration (R_{eco}) but a gradual increase in GEP over the first decades following stand replacement. Our study is in agreement with this general dynamic at least during the first 3 years after clearcutting. Annual net carbon emission was consistent over the first 3 years of study, totaling about 700 g C m^{-2} yr^{-1}, which is at the upper end of the range (200 to 850 g C m^{-2} yr^{-1}) reported after clearcutting (Amiro *et al.*, 2011). At this stage, it is unclear when the Harvard Forest clearcut site will transition from carbon source to sink at the annual scale, referred to as 'crossover time'. The Amiro *et al.* (2011) study reported a mean crossover time of about 10 years for harvested sites in North America, with warmer sites tending to have larger post-disturbance emissions and faster recovery to annual NEP>0. One useful indicator

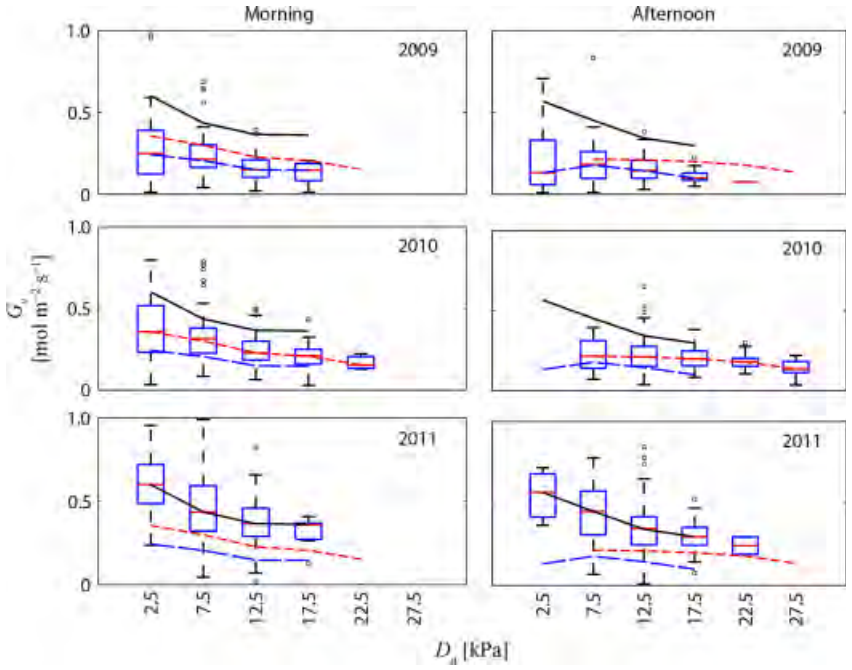

Fig. 8 Midgrowing season conductance to water vapor vs. vapor pressure deficit during morning (9:00 hours–12:00 hours) and early afternoon (12:00 hours–15:00 hours) in the 3 years post clearcutting expressed as box plots (as in Fig. 7). Curves indicate means for 2009 (blue, long dash), 2010 (red, short dash), and 2011 (black, continuous). Midgrowing season is defined as the 12th to 17th biweeks of the year.

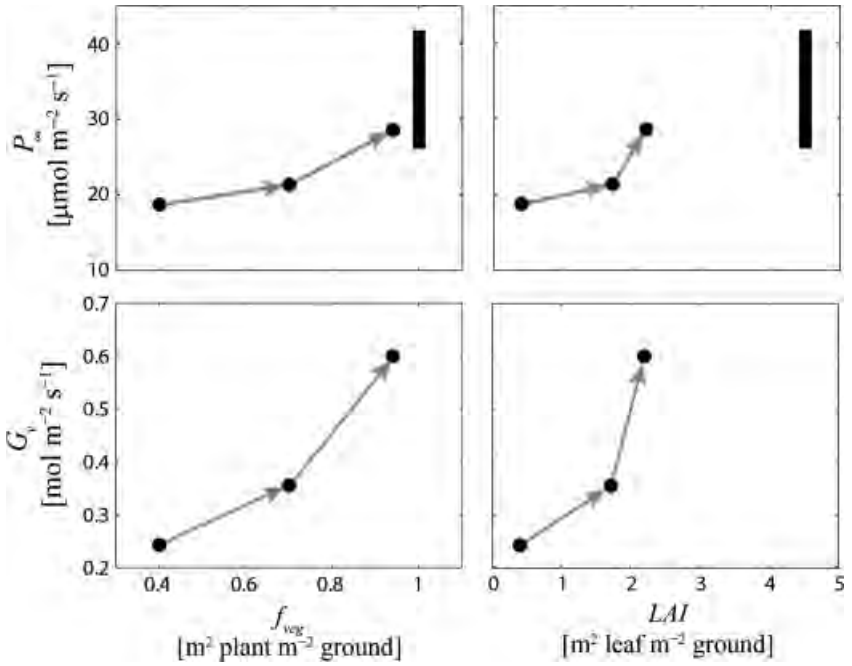

Fig. 9 Asymptotic ecosystem-scale photosynthetic rate at high light (P_∞), and maximum canopy conductance to water vapor (G_v) for morning hours and low vapor pressure deficit conditions each plotted vs. vegetation fractional cover and leaf area index during the midgrowing season. Arrows indicate flow from 2009 to 2011. Leaf area index was approximated from average leaf area per species area for the ten most abundant species (Table 2, LAI_{sp}) times total vegetation cover for all species in July of each year (Table 1). Vertical bars indicate estimates for the neighboring mature forest of the Harvard Forest Environmental Monitoring Station during the period 1992–2004 as reported by Urbanski *et al.* (2007).

of the current carbon balance status is the ratio of annual GEP to R_{eco}, which has been shown to increase from a low of 0.2–1.2 over the first 10–20 years after harvest clearing for most sites (Amiro *et al.*, 2011). In this study, we found GEP/R_{eco} of about 0.65 in the second and third years post-clearing, which exceeded the average reported by Amiro *et al.* (2011), and was consistent with a rapid recovery of plant productivity and vigorous vegetation regrowth.

The large volume of CWD and dead roots in the post-clearcut environment contribute substantially to ecosystem respiration, which again is about 1.5 times larger than annual GEP. Chamber-based measurements at our site indicate that CWD accounts for 18% of total daytime ecosystem respiration during summer months (Vanderhoof *et al.*, 2013). This is much higher than the 2.3% estimated in a nearby forest after selective logging (Liu *et al.*, 2006), though that study sampled smaller pieces of CWD just after cutting. Chamber-based soil respiration (including litter) measurements during the months of June and July indicate that it accounts for another 44% of total ecosystem respiration, leaving 36% to contributions from aboveground autotrophic respiration, meaning leaves, and stems. For comparison, Lavigne *et al.* (1997) found soil respiration to comprise a larger fraction (48–71%) of total ecosystem respiration in boreal coniferous forests, and Janssens *et al.* (2001) reported a mean of 69% across European forests, or 63% when excluding forests with recent soil disturbance. Though the soil-derived fraction of total ecosystem respiration is lower at the HF clearcut site, when CWD releases are also included, the combined estimate (62%) is more consistent with these multi-site syntheses. Comparing soil respiration measurements across years suggest a possible increase of emission over time with mean rates averaging 5.3 ± 0.3 μmol CO_2 m^{-2} s^{-1} in 2011 and 5.8 ± 0.3 μmol CO_2 m^{-2} s^{-1} in 2012 (Kappel *et al.*, 2013). This trend is consistent with the rise in GEP, which can be expected to elevate respiration through belowground supply of carbohydrates, root turnover, and litter input (Högberg *et al.*, 2001). However, a t-test indicates that plot-to-plot and date-to-date variability is large relative to the difference in means between years ($P = 0.5029$). The trenched plot experiment suggests that heterotrophic respiration accounts for about 66% of total soil respiration, with a mean midday rate of 4.1 ± 0.3 μmol CO_2 m^{-2} s^{-1} during the summer months (Kappel *et al.*, 2013). This is consistent with expectations from a meta-analysis by Subke *et al.* (2006), which indicates that the heterotrophic fraction of total soil respiration tends to decrease with forest age. This site's heterotrophic respiration rate is higher than that reported in some other studies (Tang & Baldocchi, 2005; Schuur & Trumbore, 2006), consistent with the large mass of dead biomass decomposing belowground. The root contribution (R_{root}:R_{soil}) is generally expected to range 0.3–0.5 in terrestrial ecosystems (Raich & Schlesinger, 1992; Hanson *et al.*, 2000) but has been shown to vary more widely (0.0–0.6) in a recent synthesis (Bond-Lamberty *et al.*, 2004).

Evapotranspiration recovered rapidly and continued to rise over the first 3 years in rough proportion to the rise in GEP and despite greater precipitation and soil moisture throughout much of summer of the first year post-clearcut. A corresponding decline in H was observed, and thus a decrease in the Bowen ratio (H/LE). Such shifts in surface energy partitioning would be expected to modify regional-scale boundary layer processes of convection, mixing, and cloud formation if they take place over a sufficiently large area and with appropriate spatial arrangement (Avissar & Pielke, 1989; Pielke *et al.*, 1998; Baidya Roy & Avissar, 2002). Evapotranspiration in the second and third years of recovery (483 and 517 mm yr^{-1}) was similar to, if not greater than, that measured in neighboring hemlock and red oak-dominated forests (327 and 417 mm yr^{-1}, respectively) albeit in different years (Hadley *et al.*, 2008). Thus, one should not expect a sustained increase in catchment water yield (runoff) with clearcutting when followed by rapid, vigorous vegetation regrowth. This is consistent with findings from the Florida slash pine clearcut study of Gholz & Clark (2002); however, their site experienced frequent flooding that likely supported a rapid recovery of ET. With regard to the radiation fluxes, their general stability across years during the non-snow covered season is unsurprising, and strong dependence of wintertime radiation on snow cover and associated higher albedo is to be expected. As the regrowing forest matures and vegetation continues to grow, we could expect increased shading of the snow cover and a reduction in albedo. Comparison to the radiation fluxes over a neighboring mature forest should provide a good indication of the expected long-term trend in albedo and enable calculation of the net radiative forcing from the clearcut treatment.

Seasonal patterns in GEP and ET both indicated sizable vegetation activity in the spring and autumn seasons, possibly more active than that reported for neighboring deciduous broadleaf forests and more akin to the neighboring coniferous forests (Wofsy *et al.*, 1993; Goulden *et al.*, 1996; Hadley *et al.*, 2008). Though this needs to be assessed quantitatively by comparative analysis across flux towers at the Harvard Forest, it is suggestive of earlier leaf out and later leaf senescence and drop at the clearcut site compared to the neighboring mature forests. If found to be true this runs contrary to recent work indicating a general increase in growing season length with

time since disturbance during mainly the first 20 years of stand development (Coursolle *et al*., 2012). Site-specific monitoring of weekly phenology would be ideal to determine if this is the case, but is unfortunately not available for the first years of study at the clearcut site. Satellite remote sensing of vegetation index may be a useful tool for future analysis, but preliminary exploration with MODIS normalized difference and enhanced difference vegetation indices (MOD13Q1, NDVI and EVI) was not successful due to low spatial resolution and associated difficulty in distinguishing the clearcut tract from the surrounding vegetation of mature hardwood and coniferous forests.

We were unable to determine if rises in GEP and ET can be attributed to the expansion of leaf area and vegetation cover or a change in vegetation physiology, or maybe even microclimate. Detailed, intensive monitoring of vegetation cover and composition, leaf area by species, and leaf-scale physiological function are all needed to adequately address this issue. By measuring such ecosystem attributes over time, it should be possible to estimate the role of each factor.

This study is the first of its kind to offer as detailed an account of the early temporal patterns of carbon and water fluxes following forest clearing in a temperate, deciduous broadleaf forest environment. We found rapid recovery with sustained increases in GEP over the first three growing seasons post clearing, coincident with large and relatively stable net emission of CO_2 because of sizable ecosystem respiration. Soil respiration is estimated to contribute 44% of total ecosystem respiration during summer months and coarse woody debris accounts for another 18%. ET also recovered rapidly and continued to rise across years with a corresponding decrease in *H*. Gross short-wave and long-wave radiative fluxes were stable across years except for strong wintertime dependence on snow covered conditions and corresponding variation in albedo. Further study is needed to determine the degree to which vegetation structure, composition, and function are responsible for the observed increases in GEP and ET. Continued monitoring of fluxes is needed to further document how carbon, water, and energy fluxes vary during this period of highly dynamic vegetation change. Future work should utilize the local network of flux towers to compare fluxes among contrasting land cover types of Harvard Forest, including the post-clearcut environment, mature hemlock forest, and oak-dominated deciduous broadleaf forest, with analysis of each site's unique function as it varies at seasonal, annual, and interannual scales.

Acknowledgements

We thank Audrey Barker-Plotkin, Mark VanScoy, Julian Hadley, Aaron Ellison, and David Foster of the Harvard Forest Long-Term Ecological Research Site for their assistance with site selection and characterization. We also extend thanks to numerous undergraduate research technicians for their tireless efforts in the field, including Graham Twibell, Michelle Smith, Angela Marshall, Crystal Garcia, Krittika Govil, Katharine Chute, Marcus Pasay, Alexander Kappel, and Paul Quackenbush. Thanks also to three anonymous reviewers. Major financial support for this work came from research funds to Christopher Williams from Clark University. The study was additionally supported through NASA Terrestrial Ecology award NNX10AR68G (2N041), the 2010-2011 Albert, Norma and Howard Geller '77 Endowed Research Awards for Projects Relating to Sustainability administered by the George Perkins Marsh Institute of Clark University, and the National Science Foundation (Award No. 0620443) Research Experience for Undergraduates Site award to the Harvard Forest LTER Site.

References

Amiro BD, Chen JM, Liu J (2000) Net primary productivity following forest fire for Canadian ecoregions. *Canadian Journal of Forest Research-Revue Canadienne De Recherche Forestiere*, **30**, 939–947.

Amiro BD, Orchansky AL, Barr AG *et al*. (2006) The effect of post-fire stand age on the boreal forest energy balance. *Agricultural and Forest Meteorology*, **140**, 41–50. doi:10.1016/j.agrformet.2006.02.014.

Amiro BD, Barr AG, Barr JG *et al*. (2011) Ecosystem carbon dioxide fluxes after disturbance in forests of North America. *Journal of Geophysical Research*, **115**, G00K02. doi:10.1029/2010JG001390.

Aubinet M, Grelle A, Ibrom A *et al*. (2000) Estimates of the annual net carbon and water exchange of forests: the EUROFLUX methodology. *Advances in Ecological Research*, **30**, 113–175.

Avissar R, Pielke RA (1989) A parameterization of heterogeneous land surfaces for atmospheric numerical models and its impact on regional meteorology. *Monthly Weather Review*, **117**, 2113–2136. doi: http://dx.doi.org/10.1175/1520-0493(1989)117<2113:APOHLS>2.0.CO;2.

Baidya Roy S, Avissar R (2002) Impact of land use/land cover change on regional hydrometeorology in Amazonia. *Journal of Geophysical Research*, **107**, 8037. doi:10.1029/2000JD000266.

Ball T, Smith KA, Moncrieff JB (2007) Effect of stand age on greenhouse gas fluxes from a Sitka spruce [*Picea sitchensis* (Bong.) Carr.] chronosequence on a peaty gley soil. *Global Change Biology*, **13**, 2128–2142.

Becker DR, Skog K, Hellman A, Halvorsen KE, Mace T (2009) An outlook for sustainable forest bioenergy production in the Lake States. *Energy Policy*, **37**, 5687–5693. doi:10.1016/j.enpol.2009.08.033.

Binford M, Gholz H, Starr G, Martin T (2006) Regional carbon dynamics in the southeastern U.S. coastal plain: balancing land cover type, timber harvesting, fire, and environmental variation. *Journal of Geophysical Research – Biogeosciences*, **111**, D24S92. doi:10.1029/2005JD006820.

Bond-Lamberty B, Wang C, Gower ST (2004) A global relationship between the heterotrophic and autotrophic components of soil respiration? *Global Change Biology*, **10**, 1756–1766.

Boose E (2001) *Fisher Meteorological Station (since 2001)*. Harvard Forest Data Archive: HF001. Available at: http://harvardforest.fas.harvard.edu/data-archive (accessed 25 September 2013).

Bosch JM, Hewlett JD (1982) A review of catchment experiments to determine the effect of vegetation changes on water yield and evapotranspiration. *Journal of Hydrology*, **55**, 3–23.

Brown AE, Zhang L, McMahon TA, Western AW, Vertessy RA (2005) A review of paired catchment studies for determining changes in water yield resulting from alterations in vegetation. *Journal of Hydrology*, **301**, 28–61.

Brutsaert WH (1982) *Evaporation into the Atmosphere: Theory, History, and Applications*. Kluwer Academic Publishers, Dordrecht.

Burba GG, Anderson DJ, Xu L, McDermitt DK (2006) Correcting apparent off-season CO_2 uptake due to surface heating of an open path gas analyzer: progress report

of an ongoing study. *Conference on Agricultural and Forest Meteorology*, American Meteorological Society, San Diego, CA.

Butman D, Raymond PA (2011) Significant efflux of carbon dioxide from streams and rivers in the United States. *Nature-Geoscience*, **4**, 839–842. doi:10.1038/ngeo1294.

Campbell GS, Norman JM (1998) *An Introduction to Environmental Biophysics*. Springer, New York.

Cappaert D, McCullough DG, Poland TM, Siegert NW (2005) Emerald ash borer in North America: a research and regulatory challenge. *American Entomologist*, **51**, 152–165.

Chen J, Franklin JF, Lowe SL (1996) Comparison of abiotic and structurally defined patch patterns in a hypothetical forest landscape. *Conservation Biology*, **10**, 854–862.

Chen J, Saunders CSC, Crow TC *et al.* (1999) Microclimate in forest ecosystems and landscape ecology: variations in local climate can be used to monitor and compare the effects of different management regimes. *BioScience*, **49**, 288–297.

Chen J, Paw UKT, Ustin SL, Suchanek TH, Bond BJ, Brosofske K, Falk M (2004) Net ecosystem exchanges of carbon, water, and energy in young and old-growth Douglas-fir forests. *Ecosystems*, **7**, 534–544.

Clark KL, Gholz HL, Castro MS (2004) Carbon dynamics along a chronosequence of slash pine plantations in northern Florida. *Ecological Applications*, **14**, 1154–1171.

Cohen W, Harmon M, Wallin DO, Fiorella M (1996) Two decades of carbon flux from forests of the Pacific Northwest. *BioScience*, **46**, 836–844.

Coursolle C, Margolis HA, Giasson M-A *et al.* (2012) Influence of stand age on the magnitude and seasonality of carbon fluxes in Canadian forests. *Agricultural and Forest Meteorology*, **165**, 136–148.

Eugster W, Senn W (1995) A cospectral correction model for measurement of turbulent No2 flux. *Boundary-Layer Meteorology*, **74**, 321–340.

Farley KA, Jobbagy EG, Jackson RB (2005) Effects of afforestation on water yield: a global synthesis with implications for policy. *Global Change Biology*, **11**, 1565–1576. doi:10.1111/j.1365-2486.2005.01011.x.

Ghimire B, Williams CA, Collatz GJ, Vanderhoof ME (2012) Fire-induced carbon emissions and regrowth uptake in western U.S. forests: documenting variation across forest types, fire severity, and climate regions. *Journal of Geophysical Research*, **117**, G03036. doi:10.1029/2011JG001935.

Gholz HL, Clark KL (2002) Energy exchange across a chronosequence of slash pine forests in Florida. *Agricultural and Forest Meteorology*, **112**, 87–102.

Gough CM, Vogel CS, Harrold KH, George K, Curtis PS (2007) The legacy of harvest and fire on ecosystem carbon storage in a northern temperate forest. *Global Change Biology*, **13**, 1935–1949.

Goulden ML, Munger JW, Fan S-M, Daube BC, Wofsy SC (1996) Exchange of carbon dioxide by a deciduous forest: response to interannual climate variability. *Science*, **271**, 1576–1578.

Goulden ML, Winston GC, McMillan AMS, Litvak ME, Read EL, Rocha AV, Rob Elliot J (2006) An eddy covariance mesonet to measure the effect of forest age on land-atmosphere exchange. *Global Change Biology*, **12**, 2146–2162.

Goulden ML, McMillan AMS, Winston GC, Rocha AV, Manies KL, Harden JW, Bond-Lamberty BP (2011) Patterns of NPP, GPP, respiration, and NEP during boreal forest succession. *Global Change Biology*, **17**, 855–871. doi:10.1111/j.1365-2486.2010.02274.x.

Grant RF, Barr AG, Black TA, *et al.* (2007) Net ecosystem productivity of boreal jack pine stands regenerating from clearcutting under current and future climates. *Global Change Biology*, **13**, 1423–1440.

Haack RA, Hérard F, Sun JM, Turgeon JJ (2010) Managing invasive populations of asian longhorned beetle and citrus longhorned beetle: a worldwide perspective. *Annual Review of Entomology*, **55**, 521–546.

Hadley JL, Kuzeja PS, Daley MJ, Phillips NG, Mulcahy T, Singh S (2008) Water use and carbon exchange of red oak- and eastern hemlock-dominated forests in the northeastern USA: implications for ecosystem-level effects of hemlock woolly adelgid. *Tree Physiology*, **28**, 615–627.

Hagemann U, Moroni MT, Gleibner J, Makeschin F (2010) Disturbance history influences downed woody debris and soil respiration. *Forest Ecology and Management*, **260**, 1762–1772.

Hanson PJ, Edwards NT, Garten CT, Andrews JA (2000) Separating root and soil microbial contributions to soil respiration: a review of methods and observations. *Biogeochemistry*, **48**, 115–146.

Harmon ME, Sexton J (1996) *Guidelines for Measurements for of Woody Detritus in Forest Ecosystems*. Publication No 20, US LTER Network, College of Forest Resources, University of Washington, Seattle, WA.

Högberg P, Nordgren A, Buchmann N, Taylor AFS, Ekblad A, Högberg MN, Read DJ (2001) Large-scale forest girdling shows that current photosynthesis drives soil respiration. *Nature*, **411**, 789–792.

Hsieh CI, Katul G, Chi T (2000) An approximate analytical model for footprint estimation of scaler fluxes in thermally stratified atmospheric flows. *Advances in Water Resources*, **23**, 765–772.

Humphreys ER, Black A, Morgenstern K, Li Z, Nesic Z (2005) Net ecosystem production of a Douglas-fir stand for 3 years following clearcut harvesting. *Global Change Biology*, **11**, 450–464. doi:10.1111/j.1365-2486.2005.00914.x.

Jackson RB, Randerson JT, Canadell JG *et al.* (2008) Protecting climate with forests. *Environmental Research Letters*, **3**, 044006. doi:10.1088/1748-9326/3/4/044006.

Janssens IA, Lankreijer H, Matteucci G *et al.* (2001) Productivity overshadows temperature in determining soil and ecosystem respiration across European forests. *Global Change Biology*, **7**, 269–278.

Jomura M, Komainami Y, Tamai K, Miyami T, Goto Y, Dannoura M (2007) The carbon budget of coarse woody debris in a temperate broad-leaved secondary forest in Japan. *Tellus Series B*, **59**, 211–222.

Jones MD, Durall DM, Cairney JWG (2003) Ectomycorrhizal fungal communities in young forest stands regenerating after clearcut logging. *New Phytologist*, **157**, 399–422.

Kappel A, Khomik M, Vanderhoof ME, Williams CA (2013) *Post-disturbance Soil Respiration Dynamics in a Clearcut Temperate Forest*. Honor's Thesis. Clark University, Worcester, MA.

Kashian DM, Romme WH, Tinker DB, Turner MG, Ryan MG (2006) Carbon storage on landscapes with stand-replacing fires. *BioScience*, **56**, 598–606.

Kittredge DB, Finley AO, Foster DR (2003) Timber harvesting as ongoing disturbance in a landscape of diverse ownership. *Forest Ecology and Management*, **180**, 425–442.

Kowalski AS, Loustau D, Berbigier P *et al.* (2004) Paired comparisons of carbon exchange between undisturbed and regenerating stands in four managed forests in Europe. *Global Change Biology*, **10**, 1707–1723. doi:10.1111/j.1365-2486.2004.00846.x.

Kurz WA, Apps MJ (1999) A 70-year retrospective analysis of carbon fluxes in the Canadian forest sector. *Ecological Applications*, **9**, 526–547.

Lauerwald R, Hartmann J, Ludwig W, Moosdorf N (2012) Assessing the nonconservative fluvial fluxes of dissolved organic carbon in North America. *Journal of Geophysical Research*, **117**, G01027. doi:10.1029/2011jg001820.

Lavigne MB, Ryan MG, Anderson DE *et al.* (1997) Comparing nocturnal eddy covariance measurements to estimates of ecosystem respiration made by scaling chamber measurements at six coniferous boreal sites. *Journal of Geophysical Research - Atmospheres*, **102**, 28977–28985.

Law BE, Thornton PE, Irvine J, Anthoni PM, Van Tuyl S (2001) Carbon storage and fluxes in ponderosa pine forests at different developmental stages. *Global Change Biology*, **7**, 755–777.

Law BE, Sun OJ, Campbell JL, Van Tuyl S, Thornton PE (2003) Changes in carbon storage and fluxes in a chronosequence of ponderosa pine. *Global Change Biology*, **9**, 510–524.

Law BE, Turner D, Campbell JL, Van Tuyl S, Ritts WD, Cohen WB (2004) Disturbance and climate effects on carbon stocks and fluxes across Western Oregon USA. *Global Change Biology*, **10**, 1429–1444.

Lee X, Massman W, Law B (2004) *Handbook of Micrometeorology: A Guide for Surface Flux Measurement and Analysis*. Kluwer Academic Publishers, London.

Likens GE, Bormann FH, Johnson NM, Fisher DW, Pierce RS (1970) Effects of forest cutting and herbicide treatment on nutrient budgets in the Hubbard Brook watershed-ecosystem. *Ecological Monographs*, **40**, 23–47.

Likens GE, Driscoll CT, Buso DC *et al.* (1994) The biogeochemistry of potassium at Hubbard Brook. *Biogeochemistry*, **25**, 61–125.

Litvak M, Miller S, Wofsy SC, Goulden M (2003) Effect of stand age on whole ecosystem CO_2 exchange in the Canadian boreal forest. *Journal of Geophysical Research*, **108**, 8225. doi:10.1029/2001JD000854.

Liu HP, Randerson JT (2008) Interannual variability of surface energy exchange depends on stand age in a boreal forest fire chronosequence. *Journal of Geophysical Research-Biogeosciences*, **113**, G01006. doi:10.1029/2007jg000483.

Liu HP, Randerson JT, Lindfors J, Chapin FS (2005) Changes in the surface energy budget after fire in boreal ecosystems of interior Alaska: an annual perspective. *Journal of Geophysical Research-Atmospheres*, **110**, D13101. doi:10.1029/2004jd005158.

Liu WH, Bryant DM, Hutyra LR, Saleska SR, Hammond-Pyle E, Curran D, Wofsy SC (2006) Woody debris contribution to the carbon budget of selectively logged and maturing mid-latitude forests. *Oecologia*, **148**, 108–117.

Lloyd J, Taylor JA (1994) On the temperature-dependence of soil respiration. *Functional Ecology*, **8**, 315–323.

Marc V, Robinson M (2007) The long-term water balance (1972-2004) of upland forestry and grassland at Plynlimon, mid-Wales. *Hydrology and Earth System Sciences*, **11**, 44–60.

Marshall A, Vanderhoof ME, Williams CA (2011) *Post-harvest Carbon Stocks in Woody Debris, Harvard Forest, Compared to Characteristic Harvested and Mature Forest Sites*. Honor's Thesis. Clark University, Worcester, MA.

McDonald R, Motzkin G, Bank M, Kittredge D, Burk J, Foster D (2006) Forest harvesting and land-use conversion over two decades in Massachusetts. *Forest Ecology and Management*, **227**, 31–41.

McMillan A, Goulden M (2008) Age-dependent variation in the biophysical properties of boreal forests. *Global Biogeochemical Cycles*, **22**, GB2019, doi: 10.1029/2007GB003038.

Miner R (2010) *Impact of the Global Forest Industry on Atmospheric Greenhouse Gases*. Food and Agriculture Organization of the United Nations, FAO Forestry Paper 159, Rome.

Moncrieff JB, Massheder JM, deBruin H *et al.* (1997) A system to measure surface fluxes of momentum, sensible heat, water vapour and carbon dioxide. *Journal of Hydrology*, **189**, 589–611.

Monteith JL (1965) Evaporation and environment. *Symposia Society for Experimental Biology*, **19**, 205–234.

NRCS (2010) *Natural Resources Conservation Service, United States*. Department of Agriculture. Soil Survey Geographic (SSURGO) Database for Worcester County, Massachusetts. Available at: http://soildatamart.nrcs.usda.gov (accessed 23 November 2010).

Nuckolls AE, Wurzburger N, Ford CR, Hendrick RL, Vose JM, Kloeppel BD (2009) Hemlock declines rapidly with hemlock woolly adelgid infestation: impacts on the carbon cycle of southern Appalachian forests. *Ecosystems*, **12**, 179–190. doi:10.1007/s10021-008-9215-3.

Orwig DA, Cobb RC, D'Amato AW, Kizlinski ML, Foster DR (2008) Multi-year ecosystem response to hemlock woolly adelgid infestation in southern New England forests. *Canadian Journal of Forest Research-Revue Canadienne De Recherche Forestiere*, **38**, 834–843.

Papale D, Reichstein M, Aubinet M *et al.* (2006) Towards a standardized processing of Net Ecosystem Exchange measured with eddy covariance technique: algorithms and uncertainty estimation. *Biogeosciences*, **3**, 571–583.

Pearcy RW, Ehleringer J, Mooney HA, Rundel PW (eds.) (2000) *Plant Physiological Ecology: Field Methods and Instrumentation*. Kluwer Academic Publishers, Dordrecht, The Netherlands.

Pielke RA, Avissar R, Raupach M, Dolman AJ, Zeng XB, Denning AS (1998) Interactions between the atmosphere and terrestrial ecosystems: influence on weather and climate. *Global Change Biology*, **4**, 461–475.

Poland TM, McCullough DG (2006) Emerald ash borer: invasion of the urban forest and the threat to North America's ash resource. *Journal of Forestry*,**April/May**, 118–124.

Priestley CHB, Taylor RJ (1972) On the assessment of surface heat flux and evaporation using large-scale parameters. *Monthly Weather Review*, **100**, 81–92.

Raich JW, Schlesinger WH (1992) The global carbon dioxide flux in soil respiration and its relationship to vegetation and climate. *Tellus*, **44B**, 81–90.

Randerson JT, Liu H, Flanner MG *et al.* (2006) The impact of boreal forest fire on climate warming. *Science*, **314**, 1130–1132. doi:10.1126/science.1132075.

Reichstein M, Falge E, Baldocchi D *et al.* (2005) On the separation of net ecosystem exchange into assimilation and ecosystem respiration: review and improved algorithm. *Global Change Biology*, **11**, 1–16.

Rocha AV, Shaver GR (2011) Postfire energy exchange in arctic tundra: the importance and climatic implications of burn severity. *Global Change Biology*, **17**, 2831–2841. doi:10.1111/j.1365-2486.2011.02441.x.

Schelker J, Eklöf K, Bishop K, Laudon H (2012) Effects of forestry operations on dissolved organic carbon concentrations and export in boreal first-order streams. *Journal of Geophysical Research*, **117**, G01011. doi:10.1029/2011jg001827.

Schotanus P, Nieuwstadt FTM, de Bruin HAR (1983) Temperature measurement with a sonic anemometer and its application to heat and moisture fluxes. *Boundary-Layer Meteorology*, **26**, 81–93.

Schuur EAG, Trumbore SE (2006) Partitioning sources of soil respiration in boreal black spruce forest using radiocarbon. *Global Change Biology*, **12**, 165–176.

Schwalm CR, Black TA, Morgenstern K, Humphreys ER (2007) A method for deriving net primary productivity and component respiratory fluxes from tower-based eddy covariance data: a case study using a 17-year data record from a Douglas-fir chronosequence. *Global Change Biology*, **13**, 370–385.

Smith WB, Miles PD, Perry CH, Pugh SA, Forest Resources of the United States, 2007 (2009) *Forest Resources of the United States*. Gen. Tech. Rep. WO-78, USDA, Forest Service, Washington Office, Washington, DC.

Stednick JD (1996) Monitoring the effects of timber harvest on annual water yield. *Journal of Hydrology*, **176**, 79–95.

Stoy PC, Katul GG, Siqueira MBS *et al.* (2006) Separating the effects of climate and vegetation on evapotranspiration along a successional chronosequence in the southeastern US. *Global Change Biology*, **12**, 2115–2135.

Su HB, Schmid HP, Grimmond CSB, Vogel CS, Oliphant AJ (2004) Spectral characteristics and correction of long-term eddy-covariance measurements over two mixed hardwood forests in non-flat terrain. *Boundary-Layer Meteorology*, **110**, 213–253.

Subke J-A, Inglima I, Francesca Cotrufo M (2006) Trends and mothodological impacts in soil CO_2 efflux partitioning: a metaanalytical review. *Global Change Biology*, **2006**, 921–943. doi:10.1111/j.1365-2486.2006.01117.x.

Takagi K, Fukuzawa K, Liang N *et al.* (2009) Change in CO_2 balance under a series of forestry activities in a cool-temperate mixed forest with dense undergrowth. *Global Change Biology*, **15**, 1275–1288. doi:10.1111/j.1365-2486.2008.01795.x.

Tang JW, Baldocchi DD (2005) Spatial-temporal variation in soil respiration in an oak-grass savanna ecosystem in California and its partitioning into autotrophic and heterotrophic components. *Biogeochemistry*, **73**, 183–207.

Turner MG, Romme WH, Gardner RH (1999) Prefire heterogeneity, fire severit, and early postfire plant reestablishment in subalpine forests of Yellowstone National Park, Wyoming. *International Journal of Wildland Fire*, **9**, 21–36.

Turner DP, Ritts WD, Law BE *et al.* (2007) Scaling net ecosystem production and net biome production over a heterogeneous region in the western United States. *Biogeosciences*, **4**, 597–612.

Urbanski S, Barford C, Wofsy S *et al.* (2007) Factors controlling CO_2 exchange on timescales from hourly to decadal at Harvard forest. *Journal of Geophysical Research*, **112**, G02020. doi:10.1029/2006JG000293.

Vanderhoof ME, Williams CA, Pasay M, Ghimire B (2013) Controls on the rate of CO_2 emission from woody debris in clearcut and coniferous forest environments. *Biogeochemistry*, **114**, 299–311. doi:10.1007/s10533-012-9810-4.

Webb EK, Pearman GI, Leuning R (1980) Correction of flux measurements for density effects due to heat and water-vapor transfer. *Quarterly Journal of the Royal Meteorological Society*, **106**, 85–100.

Wilczak JM, Oncley SP, Stage SA (2001) Sonic anemometer tilt correction algorithms. *Boundary-Layer Meteorology*, **99**, 127–150.

Williams CA, Collatz GJ, Masek JG, Goward S (2012) Carbon consequences of forest disturbance and recovery across the conterminous United States. *Global Biogeochemical Cycles*, **26**, GB1005, doi:10.1029/2010GB003947.

Wofsy SC, Goulden ML, Munger JW *et al.* (1993) Net exchange of CO_2 in a mid-latitude forest. *Science*, **260**, 1314–1317.

Zha T, Barr AG, Black A *et al.* (2009) Carbon sequestration in boreal jack pine stands following harvesting. *Global Change Biology*, **15**, 1475–1487. doi:10.1111/j.1365-2486.2008.01817.x.

Zhang L, Dawes WR, Walker GR (2001) Response of mean annual evapotranspiration to vegetation changes at catchment scale. *Water Resources Research*, **37**, 701–708.

Supporting Information

Additional Supporting Information may be found in the online version of this article:

Figure S1. Mean half-hourly turbulent fluxes of water (LE) and carbon dioxide Net ecosystem exchange (NEE) with wind direction in 30 degree data partitions.

Figure S2. Net ecosystem exchange (NEE) during nighttime vs. friction velocity (u^*). Data are pooled by time of year in three-month segments for the year 2010, and for six, evenly spaced data partitions of half-hourly temperatures.